

LA-UR-20-23215

Approved for public release; distribution is unlimited.

Title: Uranium-hydrogen reaction mechanism and numerical model

Author(s): Schulze, Roland K.

Intended for: Knowledge archive
Report

Issued: 2020-04-28

Disclaimer:

Los Alamos National Laboratory, an affirmative action/equal opportunity employer, is operated by Triad National Security, LLC for the National Nuclear Security Administration of U.S. Department of Energy under contract 89233218CNA000001. By approving this article, the publisher recognizes that the U.S. Government retains nonexclusive, royalty-free license to publish or reproduce the published form of this contribution, or to allow others to do so, for U.S. Government purposes. Los Alamos National Laboratory requests that the publisher identify this article as work performed under the auspices of the U.S. Department of Energy. Los Alamos National Laboratory strongly supports academic freedom and a researcher's right to publish; as an institution, however, the Laboratory does not endorse the viewpoint of a publication or guarantee its technical correctness.

Uranium-hydrogen reaction mechanism and numerical model

Roland K. Schulze

W-9, MS A122

Los Alamos National Laboratory

Los Alamos, NM 87545

rkschulze@lanl.gov

Executive Summary

Introduction

10-step Mechanism

Model Implementation

Model Analysis

Prediction for Real Surfaces and Model Calibration

Calibration by Imaging of Hydriding Surfaces

Calibration by Gas Reactor Data

Experimental Project to Provide Model Calibration

Summary

Additional models of importance and future work

Acknowledgements

Executive Summary

A simple model for hydriding at engineering uranium surfaces at ambient conditions and hydrogen gas pressures < 10 torr (to possibly a few 100s of torr) is presented. This model is based on details encompassed in the 10-step mechanism, is physically based and linked to the processes of gas delivery, reactant transport, and hydride corrosion product volume growth. The model is applicable only in the framework of the 10-step mechanism in the context that hydride corrosion is controlled initially by hydrogen ingress through defect locations at the thin oxide film on the uranium surface and not through the oxide itself, and then controlled later by the growing area available for reactant transport at the surface at and after the break-through phase of the mechanism. The model is applied to a single arbitrary site of hydride nucleation and growth at a uranium surface using only two adjustable parameters that have not been and are not easily determined experimentally: area available for hydrogen ingress at the surface defect site and the original depth of hydride nucleation. This geometric-based model relies on measured reaction rates that are dependent on the square root of pressure and the specific chemistry of the surface where gas adsorption (and reactant ingress) occurs. The square root dependence on pressure is a result of a dissociative

adsorption process. Variables in the model include hydrogen headspace pressure and the output is a given as volume of hydride corrosion generated at a single corrosion site as a function of aging time under isobaric conditions. In order to simplify the physical process, volume growth is expressed as spherical and the area available for hydrogen ingress after break-through is defined using the intersection of the spherical hydride product and the surface plane. Using this volume evolution of corrosion product at the uranium metal surface, a judgment may be made as to the end of life for that surface location.

A further refinement of the model allows simulation of gas reactor data where the consumption of hydrogen from the gas phase is tracked as solid hydride corrosion product forms (decrease in hydrogen pressure in the reactor in a non-isobaric experiment). There is some optimism that this model may be properly calibrated by comparison to experimental hydriding studies. There is some limited amount of high-fidelity gas reactor data for hydriding reactions to which this model has been applied. The quality of fits to the experimental data are excellent. An experimental gas reactor project is required to provide a full complement of data to calibrate and validate this model. It is also possible that a detailed image analysis of a large number of hydride spots in the Enhanced Surveillance Uranium Hydriding Parametric Study would be useful. This would yield three experimental distributions which could be compared directly to this or other models. First a distribution of times to break-through could be extracted. Second, the distribution of initial size of the hydride spot just after break-through would yield a measure of the span of and probability of initial nucleation depths. And third, the growth of the hydrides past the break-through time would yield verification (or not) of the growth of the hydride in break-through or bulk growth phase. Finally, the requirements for an experimental gas reactor and surface imaging project to provide calibration and validation for this model (or any other model) is outlined.

Introduction

We have developed a numerical model to help predict lifetimes of uranium parts in situations where the uranium surface is exposed to hydrogen in the gas headspace. Assessments can be made based on hydrogen pressure and on an upper limit of size of a surface breached hydride spot (volume of hydride corrosion product produced). The model assumes development of a hydride nucleus at a single arbitrary subsurface location associated with an arbitrary surface defect and follows the development of the hydride nucleus to the break-through phase and further growth to the upper limit of acceptable volume of corrosion product. The model has been developed from an understanding of the hydriding mechanism outlined below in 10 steps and measured rates of hydrogen ingress at several types (chemically) of

uranium surfaces at ambient temperature and variable pressure. The key points are 1) that the hydrides nucleate only at locations where a surface defect allows hydrogen ingress (reactant delivery) into the uranium metal subsurface (beyond the oxide), and 2) that the hydrides which eventually reach surface break-through status, nucleate and grow in the near surface (few 10s of micron depth maximum) – those beyond ~50 micron have arrested growth and never reach break-through status.

10-step Mechanism

The mechanism for hydriding reactions at engineering uranium surfaces (impure uranium with air formed complete and incomplete oxide) is described in a 10-step mechanism.

- 1) Delivery of hydrogen gas to the surface – kinetic gas theory
- 2) Adsorption of molecular hydrogen on the oxide and dissociation into atomic hydrogen
- 3) Transport of atomic hydrogen through a defect in the oxide layer (transport slow through coherent, perfect UO_2) - the defect can be a void or crack in the oxide, oxide grain boundary, chemical base metal inclusion disrupting the coherency of the oxide film, partial chemical reduction of a location of oxide (e.g. reduction by hydrocarbons), or mechanical abrasion/disruption of oxide film
- 4) Dissolution of atomic hydrogen into the metal subsurface (below oxide metal interface)
- 5) Transport in the metal to nucleation site (unknown but perhaps preexisting hydride nuclei) or super-saturation leading to spontaneous nucleation
- 6) Growth of UH_3 hydride nucleus with corresponding volume expansion
- 7) Volume expansion of metal atom density leads to buried blistering at surface (detectable by SEM imaging and probably other methods such as SPM)
- 8) The yield strength of uranium metal above the blister is exceeded, leading to blister rupture at surface and break-through phase of corrosion
- 9) Delivery of hydrogen gas to hydride break-through site now fully efficient and rapid – volume of hydride grows at bulk kinetic rate consuming underlying metal
- 10) Hydride product spalls as volume increases and this leads to pitting corrosion phenomenon

Steps 1-7 are the so-called experimentally observed “induction period” prior to hydride detection and rapid bulk growth. Overall hydrogen ingress into the surface in this period is very low since the overwhelming majority of the uranium geometric

surface is covered with a passive oxide thin film, and the only ingress points are the comparatively vanishingly small (area fraction) defect sites.

1) Gas delivery

Flux of hydrogen to the uranium surface at the pressures we are concerned with (well below atmospheric pressure), is described identically by kinetic gas behavior with the flux (f) linearly related to the pressure through,

$$f = \frac{P}{\sqrt{2\pi MRT}}$$

where M is the mass and R the gas constant.

2) Surface adsorption

Adsorption of molecular hydrogen at the surface linked to a dissociation process to produce the transport species (atomic hydrogen) is described most simply through a modified Langmuir isotherm, where the fractional surface coverage (θ) is related to the square root of the pressure through,

$$\theta = \frac{K_{ad}\sqrt{P}}{1 + K_{ad}\sqrt{P}}$$

where K_{ad} is the rate constant for adsorption. This isotherm, describing the surface coverage as a function of pressure, sets the concentration of the diffusant (atomic hydrogen reactant) at the gas-solid boundary.

3) Transport into subsurface

At ambient temperature the transport rate of hydrogen in crystalline UO_2 is believed to be quite slow (experimental numbers do not exist at ambient temperature) with the diffusion constant $D \sim 10^{-13} \text{ cm}^2/\text{sec}$ or less depending on oxide stoichiometry. For transport of hydrogen in U metal or through defects in the oxide $D \text{ (cm}^2/\text{sec)} = 0.019 \exp(-46320/RT)$ with $R = 8.314 \text{ J/mol K}$. These defects are basically short circuit paths where hydrogen passes through the normal oxide thin film into the metal subsurface at a much faster rate. The defects may be oxide pinholes, fractured oxide, abrasion removed oxide, chemical inclusions originating in the base metal and breaching the surface, oxide grain boundaries, substoichiometric oxide from thermal or chemical processes, and incomplete oxide at high energy features such as edges, corners, and base metal voids and cracks. The rate of hydrogen ingress at these defect sites is controlled by 1) the gas delivery rate at the defect site (gas pressure), 2) the effective area of the defect site at the gas-solid boundary, and 3) the transport rate into the subsurface.

The first three steps can be depicted as shown in figure 1.

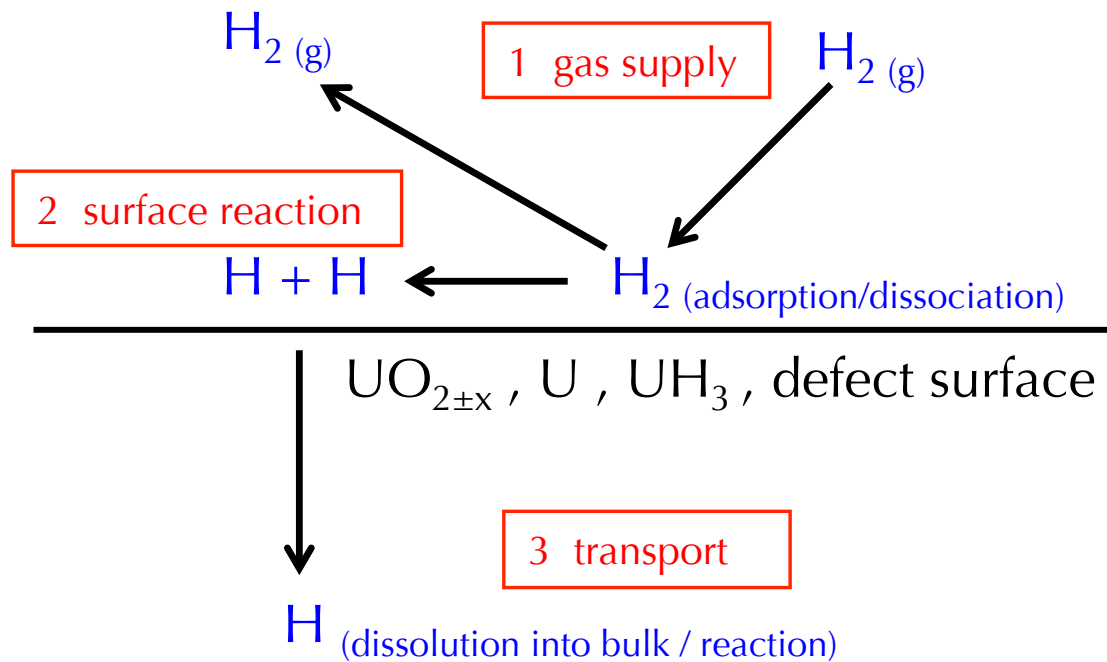


Figure 1. Depiction of first 3 steps in hydriding process. Experimental work shows that there is a transition in saturation between 1 and 10 torr of hydrogen on U metal and UH_3 surface. The measured effective sticking coefficient at 1 torr is greater than at 10 torr suggesting that at 1 torr the active sites are not yet saturated at equilibrium adsorption, but at 10 torr they are. This indicates a rate limiting process of dissociation or transport.

4) Dissolution of hydrogen into the metal subsurface

We absolutely understand that in hydriding at normal (not specially prepared surfaces) engineering uranium, the nucleation and subsequent growth of the hydride volume is in the metal subsurface and not at the oxide metal interface. Furthermore, various studies indicate the hydride nucleation locations are primarily intra-granular. Thus, the reactant (atomic H diffusant) must first dissolve into the metal before reaching the nucleation site.

5) Transport through U metal to nucleation site

For transport of hydrogen in U metal driven by a concentration gradient, $D \text{ (cm}^2\text{/sec)} = 0.019 \exp(-46320/RT)$ with $R=8.314 \text{ J/mol K}$. The simplest assumption to make here about the nucleation site is that it is pre-existing. The exact natures of the important sites are not fully known, but pre-existing UH_3 hydride nuclei (present from the original material processing) are likely locations.

6) Growth of hydride nucleus

The growth rate of the hydride nucleus depends, at first order, on the rate of hydrogen delivery to the site

Rate I

$$\text{Rate} \left(\frac{\text{moles } \text{UH}_3 \text{ formed}}{\text{cm}^2 \text{ sec}} \right) = 1.3 \times 10^{-7} \sqrt{P(\text{torr})} - 6.3 \times 10^{-8} \quad \text{for pressure} > 1 \text{ torr}$$

and

$$\text{Rate} \left(\frac{\text{moles } \text{UH}_3 \text{ formed}}{\text{cm}^2 \text{ sec}} \right) = 6.9 \times 10^{-8} \sqrt{P(\text{torr})} \quad \text{for pressure} < 1 \text{ torr}$$

7) Volume expansion of growing UH₃ hydride

This is a complex problem since the growing subsurface hydride nucleus performs an enormous amount of work on the surrounding metal in a 3-dimensional compressive strain field since the hydride phase results in a U atom-density volume expansion of 74% relative to the metal (α -U 19.1 g/cm³, 80.3 mmol U atoms/cm³ and UH₃ 11.1 g/cm³, 46.1 mmol U atoms/cm³). This in turn dramatically affects the rate of transport of hydrogen to the hydride location, with the transport rate dropping by an order of magnitude or more for highly worked metal (Condon). Thus, this step links closely to step 6). Several assumptions can be made to simplify this problem. First, we can understand that growth of deep hydrides will be arrested due to the surrounding strain field. Second, shallow hydrides will continue to grow in a relaxed strain situation by causing plastic deformation (tensile strain) in the overlying metal, and ultimately resulting in blister formation that has been observed experimentally in numerous high magnification surface hydriding studies. Finally, the depth boundary between the deep arrested growth and the shallow continued growth leading to blister formation, can be estimated by measuring the size of the hydride nucleus when it reaches the break-through phase. Based on analysis of a large number of images collected by SEM and optical means of the surface of hydrided U, this can range from 5 – 40 μm and seems to depend on the pedigree of the uranium and the surface preparation. From this, the boundary can be estimated at a few 10s of micron in depth, with, at a first approximation, nuclei deeper than $\sim 50 \mu\text{m}$ being arrested in growth.

8) Hydride break-through phase

For the shallow growing hydride nuclei (<50 μm in depth), the initial plastic deformation of the overlying α -U metal, expressed as surface blister formation, eventually reaches the ultimate tensile strength of the metal and causes rupture of the metal (and any overlying oxide layers). Now the hydride nucleus UH₃ is exposed

directly to the gas headspace and gas delivery becomes directly dependent on this greater exposed area. Again, to a first approximation, the exposed area at the time of rupture can be determined by some fraction of depth of initial nucleation. Thus, a hydride nucleus initiating at a 30 μm depth breaches the surface originally as the surface of a 30 μm sphere intersecting the surface. Only at this point is the so called "induction period" observed in uranium hydriding reaction experiments complete.

9) Direct delivery of hydrogen – volume growth of hydride at bulk kinetic rate

Rate II

Hydride product is now exposed as an equatorial cross section through the spherical nucleus (hemispherical-like morphology with an exposed areal circle at the surface for smooth surfaces, and which may be modified at real surfaces where the surface roughness is of the same order of size as the break-through diameter). The growth rate of the hydride location now depends, at first order, on the rate of hydrogen gas delivery to the site, and also again on the exposed area of that hydride spot based on the following.

$$\text{Rate} \left(\frac{\text{moles } \text{UH}_3 \text{ formed}}{\text{cm}^2 \text{ sec}} \right) = 7.8 \times 10^{-8} \sqrt{P(\text{torr})} - 1.6 \times 10^{-8} \quad \text{for pressure} > 1 \text{ torr}$$

and

$$\text{Rate} \left(\frac{\text{moles } \text{UH}_3 \text{ formed}}{\text{cm}^2 \text{ sec}} \right) = 6.3 \times 10^{-8} \sqrt{P(\text{torr})} \quad \text{for pressure} < 1 \text{ torr}$$

Reaction occurs ($3\text{H} + \text{U} \rightarrow \text{UH}_3$) and additional UH_3 material added at the hemispherical interface between the hydride and the underlying metal. Thus, the hydride spot grows in diameter and volume.

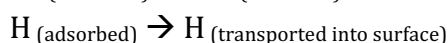
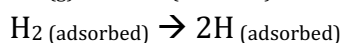
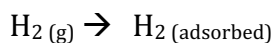
10) Hydride volume increases, leading to pitting corrosion

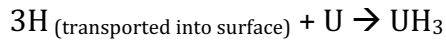
As reactions proceed at the bulk kinetic rate driven by an increasing area available for hydrogen delivery, an unconstrained (or partially or poorly constrained) hydride spalls corrosion product, changing the delivery morphology and leading to the formation of corrosion pits.

The overall process can be described chemically through the following.



This overall reaction can be described by several pertinent processes:





Note that the overall reaction contains processes related to gas delivery to the surface and adsorption through specific physical mechanism and process, dissociation of the hydrogen molecule, transport of the atomic hydrogen into the subsurface, and reaction with uranium to form the hydride. This general process holds for both the case where the transport past the oxide occurs at defect sites (mechanism steps 3-6) or at an exposed hydride in break-through phase (mechanism steps 8-10). Only the real rates are different, primarily due to differences in the area available for reactant (hydrogen) ingress.

Model Implementation

The overall situation for engineering uranium surfaces is captured in figure 2. Here a surface cross-section is shown that depicts a variety of surface defects and growing hydride nuclei, including a simplified depiction of the break-through phase morphology. At a single given nucleation site, the observed rate of hydride creation is dependent both on the rate mode (ingress through defect or at UH₃ covered metal) and the exposed area available for ingress. When the subsurface hydride nucleus is still growing, the extent of reaction is controlled by rate I and a nominally small area available for hydrogen uptake at the defect site. Once the growing nucleus achieves break-through phase, hydrogen delivery rate II comes into effect, and the area is much larger and grows at a substantial rate as the hydride grows. It is in this way that the corrosion rate accelerates once break-through phase is achieved. Deep hydrides do not lead to a break-through phase because the reactant delivery rate (atomic hydrogen) is lower through the metal due to a greater distance from the source, and due to the increasing 3-dimension compressive strain field effect, which will eventually arrest the growth of these deep hydrides.

For a given single hydride site, the poorly understood factors in this mechanism and the model that follows are:

- 1) Specific chemical or structural nature of the subsurface nucleation site
- 2) Role of the specific nature of the surface of the U metal (e.g. presence and thickness of a work hardened metal layer, or nature of surface oxide)
- 3) Nature of the surface defect site(s) allowing hydrogen ingress
- 4) Area of the defect site at the surface available for hydrogen ingress
- 5) Original depth of the subsurface nucleation site, and the critical depth required for arrested growth of the hydride nucleus

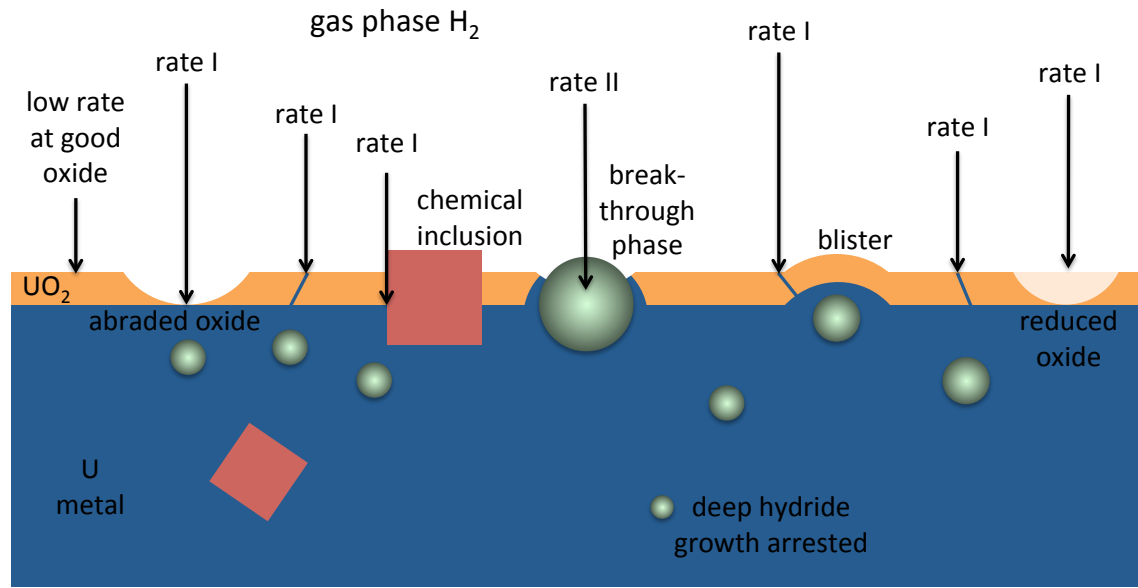


Figure 2. Stylistic depiction of an engineering uranium surface (blue U metal) in cross-section with a thin oxide layer (orange UO_2) incompletely covering the surface. Green spheres depict growing UH_3 hydride nuclei. Various types of defect sites are shown. Rate I refers to the rate of hydrogen ingress (reaction) for hydrogen at bare metal, and rate II refers to hydrogen ingress at UH_3 . From left to right the rate at good oxide coverage is very low, rate I at abrasion removed oxide, rate I at an oxide grain boundary, rate I at a chemical inclusion breaching the oxide, rate II at a UH_3 nucleus having grown to the break-through phase, rate I at a grain boundary feeding a hydride nucleus which is in the blister stage, rate I at a grain boundary feeding a deeper growing hydride nucleus, and rate I at a location where the oxide stoichiometry has been reduced. Growth of a deep hydride is arrested due to 3-dimensional strain field developing around nucleus. The extent of each reaction as a function of time (extent of hydrogen feed) is governed by the rate and the specific surface area exhibited by each defect site.

The simple model used here uses two rate expressions for formation of UH_3 product in the hydriding reaction. The first is the rate of reaction when the subsurface hydride has only first nucleated or is still growing in the subsurface. This rate encompasses all processes in steps 1-7 of the 10-step mechanism, and so it captures variables such as the hydrogen gas headspace pressure and the area at the surface presented by the defect site. The rate captures factors such as transport rate automatically and assumes that delivery of hydrogen to the forming hydride through a specific defect is controlled by the two variables. The second is the rate of reaction when the (previously) subsurface hydride has reached the break-through phase. This rate encompasses processes in steps 8 and 9 of the 10-step mechanism, and once again depends upon the hydrogen gas headspace pressure and the area at the surface presented by the break-through hydride. This area is determined

originally by the depth of the original hydride nucleus. This rate expression captures the rate of transport of hydrogen to the metal through an over layer of UH_3 hydride product and is once again controlled by the gas headspace pressure and the increasing area at the surface presented by the growing hydride product. It is clear that there is suddenly a change in growth mode at the point that the hydride nucleus breaks the surface. The intrinsic change in rate in the reaction is not very important, but the change in the surface area available for hydrogen ingress and ultimate reaction at that given site is enormous.

Model details and assumptions:

- Assumes that transport of reactant through a coherent UO_2 layer is slow and does not participate in reactant delivery.
- Determines growth of hydride only a single arbitrary nucleation site which is fed reactant through a defect site of fixed area at the surface.
- Uses a rate determined experimentally for hydrogen ingress (leading to reaction) at a bare U metal surface and for defect sites and a different rate determined experimentally for hydrogen ingress at a UH_3 covered U metal surface.
- Hydride nucleus grows in subsurface from the predetermined depth in a spherical form.
- When top of growing spherical subsurface hydride intersects the metal surface (based on the original depth of nucleation) then delivery is determined by the area formed by the intersection of the growing sphere and the surface plane. This is the start of the break-through phase.
- Model contains two adjustable parameters: 1) original depth of nucleation, and 2) the original area available for hydrogen ingress presented by the defect at the surface.
- Model contains one variable: the hydrogen gas headspace pressure.

Figure 3 shows a depiction of a surface cross section at a single given nucleation site and the time progression of the model as formulated from the point of early nucleation (t_0) through to the full break-through phase (t_3). The important thing to note is that the mechanism of hydrogen delivery, and thus the hydride growth rate, changes once the subsurface hydride reaches break-through.

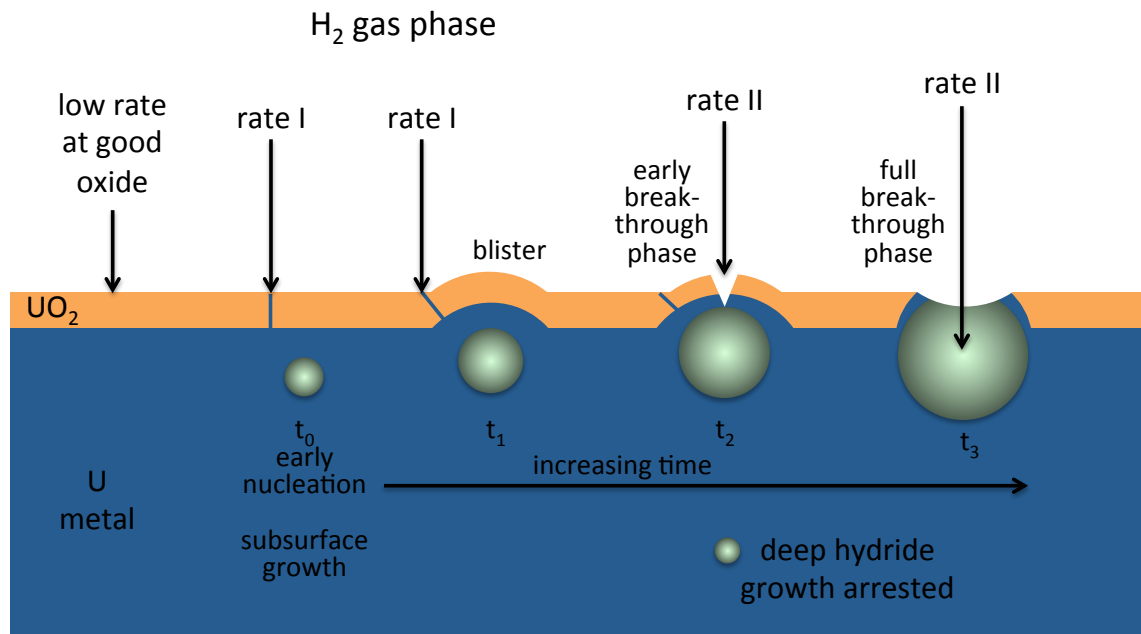


Figure 3. Stylistic depiction of an engineering uranium surface (blue U metal) in cross-section with a thin oxide layer (orange UO_2) covering the surface. Green spheres depict a growing UH_3 hydride nucleus. Time progression of this hydride growth is shown based on the mechanism. Early nucleation at t_0 with subsurface growth of hydride fed by hydrogen ingress at defect in oxide. Blister formation at t_1 with hydrogen feed still at defect. Initial break-through phase with hydride exposure at blister top at t_2 . Full break-through phase at t_3 with large area of hydride exposed and further growth at rate II. Growth of a deep hydride is arrested due to 3-dimensional strain field developing around nucleus.

The numerical formulation of this simple model is shown in figure 4. The model continues to have physical rigor in regards to the process of hydriding as understood from the 10-step mechanism, but there are some simplifications made in order to streamline the calculation. First, the spherical growth during the subsurface phase is likely to be reasonably correct. As discussed previously, compressive strain in the surrounding metal beneath the nucleation point prevents excessive growth in that direction while plastic deformation of the overlying metal allows expansion of the growing corrosion product. The model however, does not take into account the deformation of the overlying metal associated with the blister formation. During the break-through phase, the model assumes this point is first reached when the diameter of the growing spherical corrosion product intersects the surface. Further growth causes the area available for hydrogen ingress to be defined by the geometric intersection of the growing hydride sphere and the original surface plane. This is clearly a simplification, because at this point the hydride growth will occur laterally across the surface as well as into the surface

(normal to the surface plane), and no longer in a perfectly spherical fashion. The model also does not account for the major disruption of the metal (deformation and tearing) at the corrosion site as the hydride product volume grows.

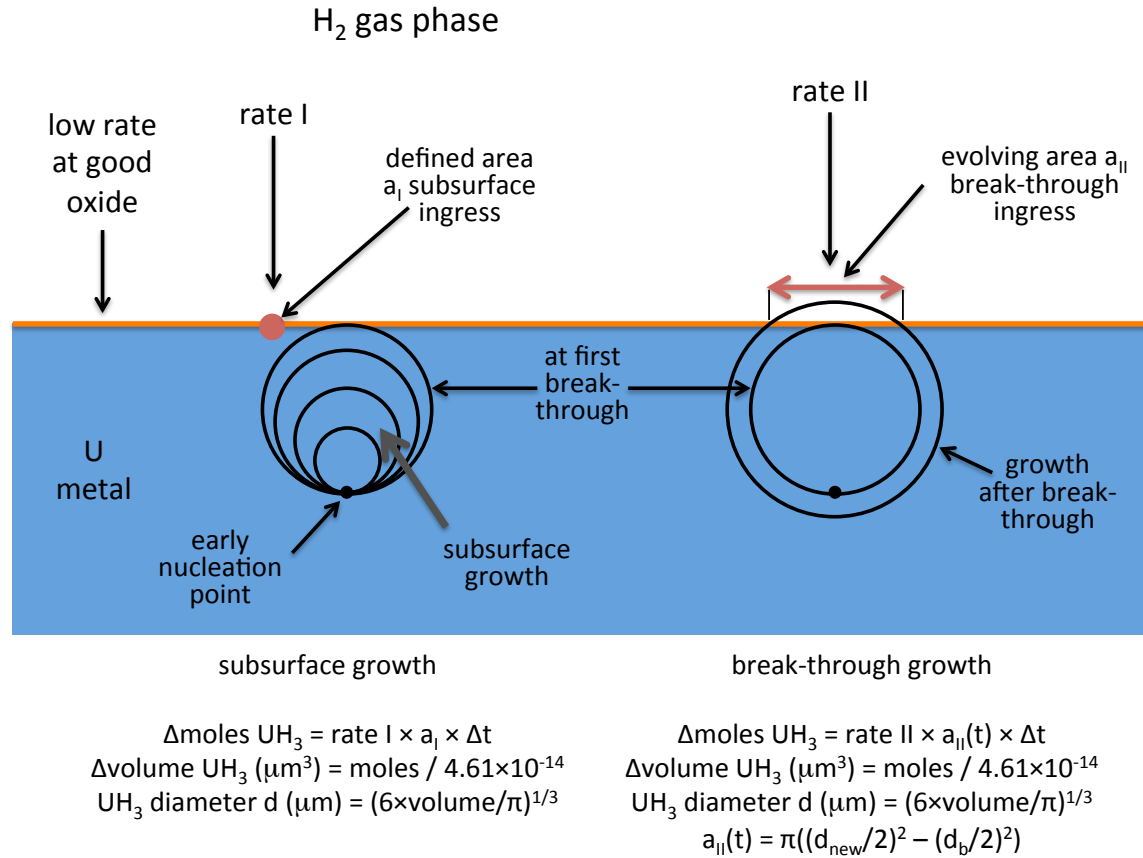


Figure 4. Formulation of the model with an understanding of a change in the mechanism between subsurface growth of hydride and break-through growth of hydride. In initial subsurface growth the volume of hydride grows linearly with time at constant pressure as the ingress site area a_I at the defect is defined and invariant. After break-through the spherical hydride continues to grow but now hydrogen delivery to the reaction site is through a constantly increasing area a_{II} . d_b is the diameter at of the subsurface hydride volume at the point of break-through and d_{new} the evolving diameter of the spherical volume of generated hydride product.

Typical results of the numerical model are shown in figure 5 for three different hydrogen gas headspace pressures. These results show the salient features in the behavior of the model which parallel behavior seen experimentally in uranium coupon hydriding experiments. The original hydride nucleation site starts off with infinitely small volume and grows quite slowly under rate I, and a vanishingly small

defect site area available for hydrogen ingress. The rate of growth is influenced by the square root of hydrogen gas pressure. At a low pressure and a reasonably small defect area the slow growing subsurface hydride stays in the blister phase for a long extended time period. At higher pressures, the blister growth is more rapid and the break-through phase is reached sooner. Once the break-through phase is achieved, the surface area available for hydrogen delivery is dramatically increased and continues to grow as the volume of hydride grows from reaction. Now the volume of hydride formed is initially at microscopic amounts but grows much more rapidly and eventually reaches macroscopic volumes (1-10 mm³).

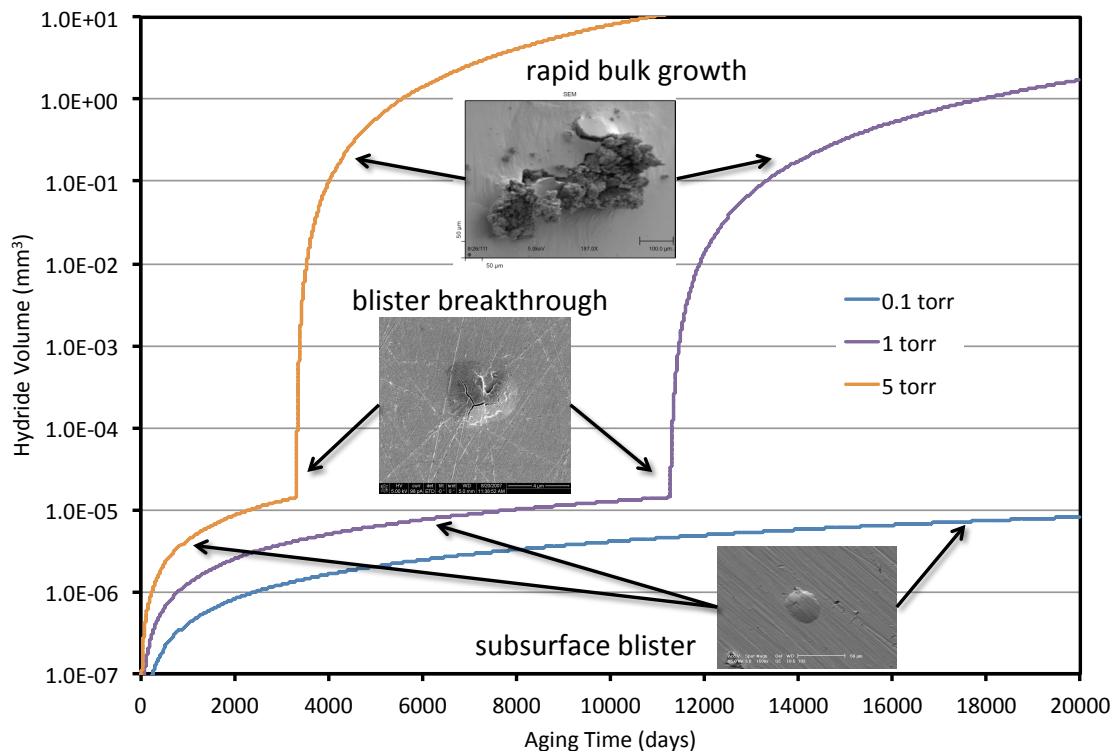


Figure 5. Results of model showing growth of hydride volume as a function of aging time at three different hydrogen gas headspace pressures. Initial conditions are depth of nucleation = 30 μm and area of defect site = 0.01 μm^2 . Note that at a H_2 pressure of 0.1 torr the subsurface hydride blister never reaches break-through in 20000 days (55 years). In the case of 1 and 5 torr H_2 pressure, the metal overlying the blister eventually cracks and the reactant delivery and subsequent growth mode changes, leading to rapid bulk growth of hydride. SEM images from coupon hydride studies are shown for three critical phases: early subsurface blister, blister at initial break-through, and full break-through phase with rapid growth.

In the initial nucleation and blister phase (prior to break-through) the volume of hydride formed increases linearly with time due to constant deliver of hydrogen

from the gas phase and constant area at the defect site available for reactant ingress. After break-through, the hydride volume growth rate proceeds closely as time² because the area available for hydrogen ingress at the break-through site is related to the size of the growing hydride volume through a square power dependence modified slightly by model details at the break-through site.

Figure 6 presents a sensitivity analysis of the model as applied through adjustment of the two parameters, original defect site area and original nucleation depth, and variation in pressure. The “standard” parameters around which we investigate sensitivity of the model are based on specific data garnered from experimental or engineering evaluations and best estimates based on observed behavior in uranium coupon hydriding studies. These are a hydrogen gas pressure of 1 torr, original nucleation site depth of 30 μm , and a surface defect site area feeding the subsurface hydride nucleus of 0.001 μm^2 (32x32 nm area).

The model shows that the volume growth of the subsurface hydride (blister and earlier) does not depend on the depth of original nucleation (top plot). This is probably not strictly true in real physical sense, but is captured this way in the model because the rate expression captures all the processes from gas phase adsorption through reactant transport to reaction to form the hydride in a single expression, controlled primarily by the presence of the short circuit path for the reactant through the passive oxide layer. All other factors such as depth are not rate limiting. Note that at 50 and 40 μm nucleation depths, the growing hydride never makes it to the break-through phase in the time frame investigated. The hydride product simply does not become large enough to breach the surface. At increasingly shallower nucleation depths the break-through phase comes earlier and with smaller hydride volume growth, and the rapid bulk growth of the hydride volume occurs sooner. The variation in hydride growth with pressure (middle plot) shows an expected dependence on pressure in both the subsurface and the break-through phases as a result of the intrinsic rate expressions exhibiting a square root dependence on pressure. Here the delivery rate of hydrogen to the surface site (defect or break-through) is of primary importance. At low hydrogen pressures (0.1 and 0.2 torr) the subsurface hydride never reaches break-through phase over the time period examined, although it is clear that the growth rates are different for the two. At higher hydrogen pressures, the subsurface growth rates continue to increase, and thus the break-through volume (for a constant original nucleation depth) is reached sooner as a function of pressure.

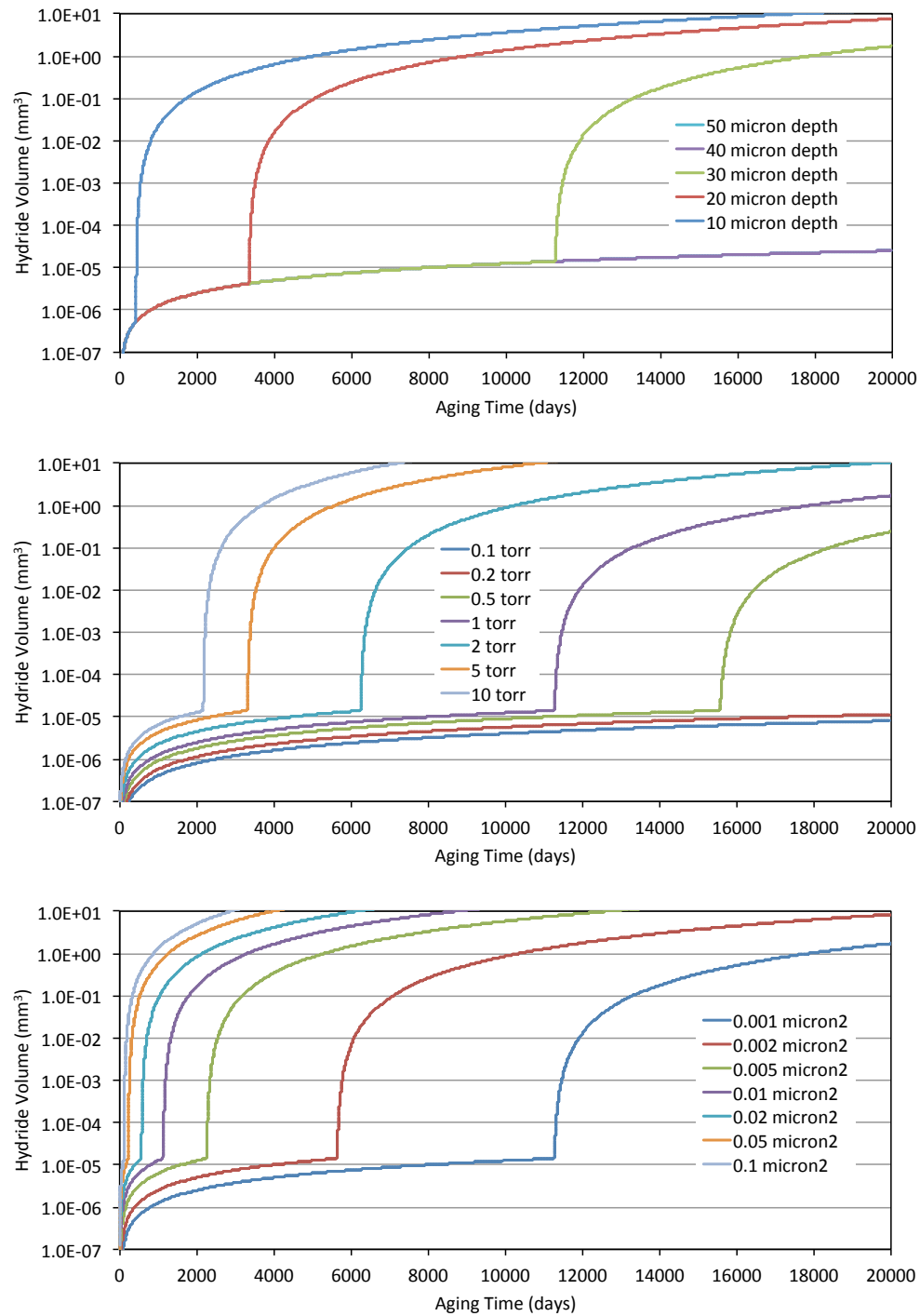


Figure 6. Sensitivity examination for the numerical model. Standard values for the variables are 1 torr hydrogen gas pressure, 0.001 μm^2 area for defect site, and 30 μm original nucleation depth. Plots of hydride volume generated as a function of aging time. Top plot shows changes in behavior with original nucleation depth. Middle plot shows changes in behavior with hydrogen gas pressure. Bottom plot show changes in behavior with area of original defect site available for hydrogen ingress.

This relationship exhibits a power law dependence influenced by the delivery of reactant dependent on the square root of pressure and the spherical volume growth of the hydride product. The time to break-through in days is $t_b = 10119 \times \text{torr}^{-0.70}$ for these given conditions. In this case, the sooner the hydride reaches break-through phase, the faster it grows in this phase. Finally, the variation of hydride growth volume with defect site area is shown in the bottom plot. With increasing area available for hydrogen ingress to the reaction site, the hydride growth increases in both the subsurface growth phase and the break-through phase. The relationship between hydride growth to time to break-through and available surface area is a weak power law dependence. The time to break-through $t_b = 10.4 \times \text{torr}^{-1.006}$ for these conditions. Once again, in this case, the sooner the hydride reaches break-through phase the faster it grows in this phase.

Model Analysis

The primary purpose of this simple model is to provide a means to understand hydriding behavior at arbitrary hydriding locations as a function of the headspace hydrogen gas pressure. In this way it becomes possible to set upper bounds on H_2 pressure for a specific desired lifetime of a given surface location with specific characteristics. While the model is based on physically real processes associated with the 10-step mechanism, it suffers from the use of two adjustable parameters that are not well understood or determined for engineering surfaces. These are the initial distance of nucleation from the uranium first surface (the nucleation depth), and the area available for hydrogen ingress associated with the defect site. Further, it suffers from a lack of fidelity associated with other processes such as a detailed accounting of work hardening in the uranium changing reaction rates, the deformation of the metal overlying the subsurface growth (the blister) leading to changes in fine dimension, and non-idealities in hydride volume growth (non-spherical) in the subsurface and break-through phases. Implementation of a finite element approach may add this fidelity, but at the cost of intensive computation. Nevertheless, the model does capture the broad mechanistic behavior observed in coupon hydriding experiments – the so called “induction time” where there is no hydriding observable and the rapid hydriding phase where gas phase hydrogen consumption increases in rate and the hydride corrosion product increases in volume at the surface. In the model these are the subsurface growth and break-through phases respectively.

Note once again that this model predicts behavior only at a single arbitrary nucleation point and not global behavior across a microscopically non-homogeneous engineering uranium surface. We do have some basis for understanding metrics of the two adjustable parameters. The depth of initial

nucleation is estimated based on three observations from a variety of experimental observations in coupon hydriding experiments. First, the size of blisters associated with the subsurface growth prior to break-through can be used to estimate the realistic range of initial nucleation depth. Second, the size of the break-through phase at first detection gives a good estimate of the initial nucleation depth to first order (perhaps to a factor of 2). Third, the ruptured metal thickness observable just past the break-through point gives us some understanding of the original metal over layer thickness (over the nucleation point). This gives us a range of depths of possibly 5-40 μm for initial nucleation eventually reaching a detectable break-through phase. It is believed that nucleation deeper than 50 μm will either take too long to grow to a detectable break-through or the growth will be arrested due to a 3-dimensional compressive strain field around the growing hydride nucleus (74% volume expansion!). Understanding the area available for hydrogen ingress at a specific defect site is a more difficult problem. Almost certainly, this will be a rather broad distribution of possibility, encompassed by the variety of defects which will participate. A broad estimate is provided by considering the following. The defects where hydrogen ultimately finds its way into the metal subsurface are inhomogeneities in the passive oxide over layer. First, if one considers defects not associated with major surface disruption such as in-situ abrasion removal of oxide, then this leaves us with pinholes in the oxide, oxide grain boundaries, and discontinuities in the oxide associated with chemical inclusions. The hydrogen ingress points in a local sense in this range are on the order of 10s of nm in spatial extent. In a conservative sense then a local defect may be $0.1 \times 0.1 \mu\text{m}$ leading to an effective area for ingress of $0.01 \mu\text{m}^2$. For the purposes of this model and analysis, in order to span this range we consider areas over several orders of magnitude from 0.001 to $0.1 \mu\text{m}^2$. Major surface disruptions may also exist in a real engineering sense where hydrogen ingress occurs over much broader areas due to oxide abrasion, chemically reduced oxide, or other processes leading to ingress paths not yet known. In this case the induction period is effectively bypassed by providing a large area for reaction initially, similar to the area provided at initial break-through in the normal sequence of events. The only difference being is that this area is also constant and not growing until break-through occurs.

One possible useful metric in applying this model to evaluate lifetimes of real engineering uranium surfaces is the time to break-through. This parameter is useful because, in a real sense, this signals the transition between low rate growth of hydride in the subsurface and much more rapid grow of hydride on and external to the surface. In addition, this metric is easy to identify in the model and possibly also experimentally as the time of first detection of a microscopic hydride spot.

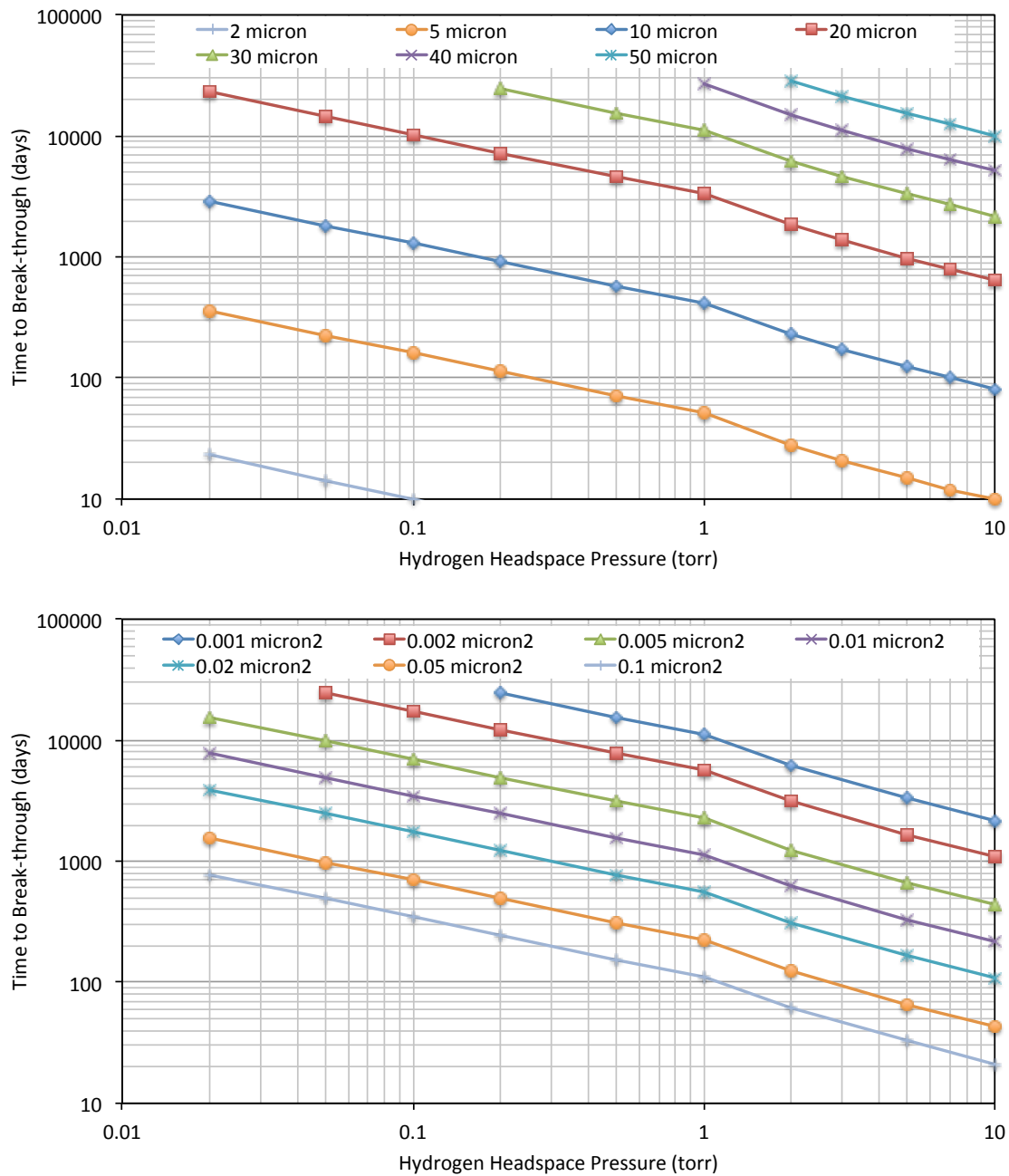


Figure 7. Plots of time to break-through as a function of hydrogen headspace pressure based on the model. Top plot shows a family of curves with defect area set to $0.001 \mu\text{m}^2$ and variation in nucleation depth. Bottom plot shows a family of curves with nucleation depth set to $30 \mu\text{m}$ and variation in defect area.

Figure 7 shows the variation in time to break-through with hydrogen headspace pressure. The top plot shows a family of curves describing the case of $0.001 \mu\text{m}^2$ initial defect area and variation in depth of nucleation. The bottom plot shows a

family of curves describing the case of 30 μm nucleation depth and variation in initial area of the hydrogen ingress defect area. From these curves, one might pick out time to break-through (an effective lifetime perhaps) as a function of pressure for variation over some span of the adjustable parameters.

Prediction for Real Surfaces and Model Calibration

A full analysis of engineering uranium surfaces to determine depth distributions of just-nucleated hydride locations, and some measure of the distribution of areas of hydrogen ingress defects sites would be useful as a means apply realistic physical parameters to the model. These measurements are quite difficult as the full nature of important defects is not fully understood, detection and measurement of just-initiated hydrides in the metal subsurface is required, and the size scales of the important sites are very small. In any case, positional prediction of hydriding corrosion at a uranium surface and not just an arbitrary, isolated nucleation site requires a detailed understanding of the microscopic nature of that surface and subsurface.

Calibration by Imaging of Hydriding Surfaces

There is some optimism that this model (or others) may be properly calibrated by comparison to experimental hydriding studies where relevant material and surface conditions have been used and the reaction conditions are of the correct nature. The calibration required is an understanding of the distribution (span and probability) of the two primary adjustable parameters: the initial surface defect area available for hydrogen ingress and the initial depth of nucleation, since, as shown above the values of these parameters dramatically influence the volume growth of hydride product with time. In particular, a detailed image analysis of a large number of evolving hydride spots in the Enhanced Surveillance Uranium Hydriding Parametric Study would be useful. This would yield three experimental distributions and growth rates which could be compared directly to this and other models:

- 1) Distribution of time to break-through could be extracted. This is the microscopic visual identification of hydride product at the surface at a given location.
- 2) Distribution of initial size of the hydride spot just after break-through. This would yield a measure of the span of and probability of initial nucleation depths.
- 3) A measure of the growth of the hydrides past the break-through time would yield verification (or not) of the growth of the hydride in break-through or bulk growth phase.

There is a huge amount of data available in the form of uranium surface images generated by the Parametric Study under conditions of nominal interest, with some variation in materials surface, configuration, and headspace gas pressure for ambient temperature. These images exist as a function of aging time (hydriding time) for an extended time period. What is required is image analysis of a large number of individual hydride locations in order to generate distributions of growth behavior. It is probably important to employ local LANL expertise in image analysis and image analysis automation in order to extract the details listed above.

Calibration by Gas Reactor Data

This model is also simply extended to analyze typical gas reactor data (not isobaric) by tracking hydrogen gas moles consumed instead of moles of corrosion product produced. In this case the model parallels a hydriding reactor experiment, where, at zero time, a reactor containing a uranium sample is filled with some set pressure of hydrogen. The hydrogen reacts with the uranium surface and the headspace pressure decreases in accordance with processes in the 10-step mechanism. In the model the headspace hydrogen pressure is tracked with each time step and this new pressure is used in the rate equation. The concepts of hydrogen ingress at the original area defect and the further ingress at an increasing site area after break-through remain the same.

An additional sensitivity examination is shown in figures 8 and 9. The additional new parameters required in a gas consumption process are the starting pressure and the number of nucleation sites for the given uranium surface. Figure 8 shows the behavior with variation in initial reactor hydrogen pressure. Note that at higher pressure, the break-through phase is reached sooner and then pressure decreases with a linear mid-section in each case until the hydrogen delivery rate (pressure) becomes vanishingly small. Figure 9 shows behavior with variation in number of nucleation sites. For given identical nucleation sites, the break-through time is identical in each case, but the rate of hydrogen uptake by the solid (disappearance from the gas phase) is modified by a factor equal to the number of nucleation sites. In this way then the model can be related to measurable parameters in a gas reactor experiment. The bottom plots in figures 8 and 9 show an expanded ordinate in order to examine behavior in the subsurface growth phase (induction period) prior to break-through growth. Note that the gas consumption is quantitatively shown and is linear as expected from the model. The gas consumption with time is not zero in this induction period, and may be a measurable quantity in an experimental gas reactor apparatus under the correct conditions.

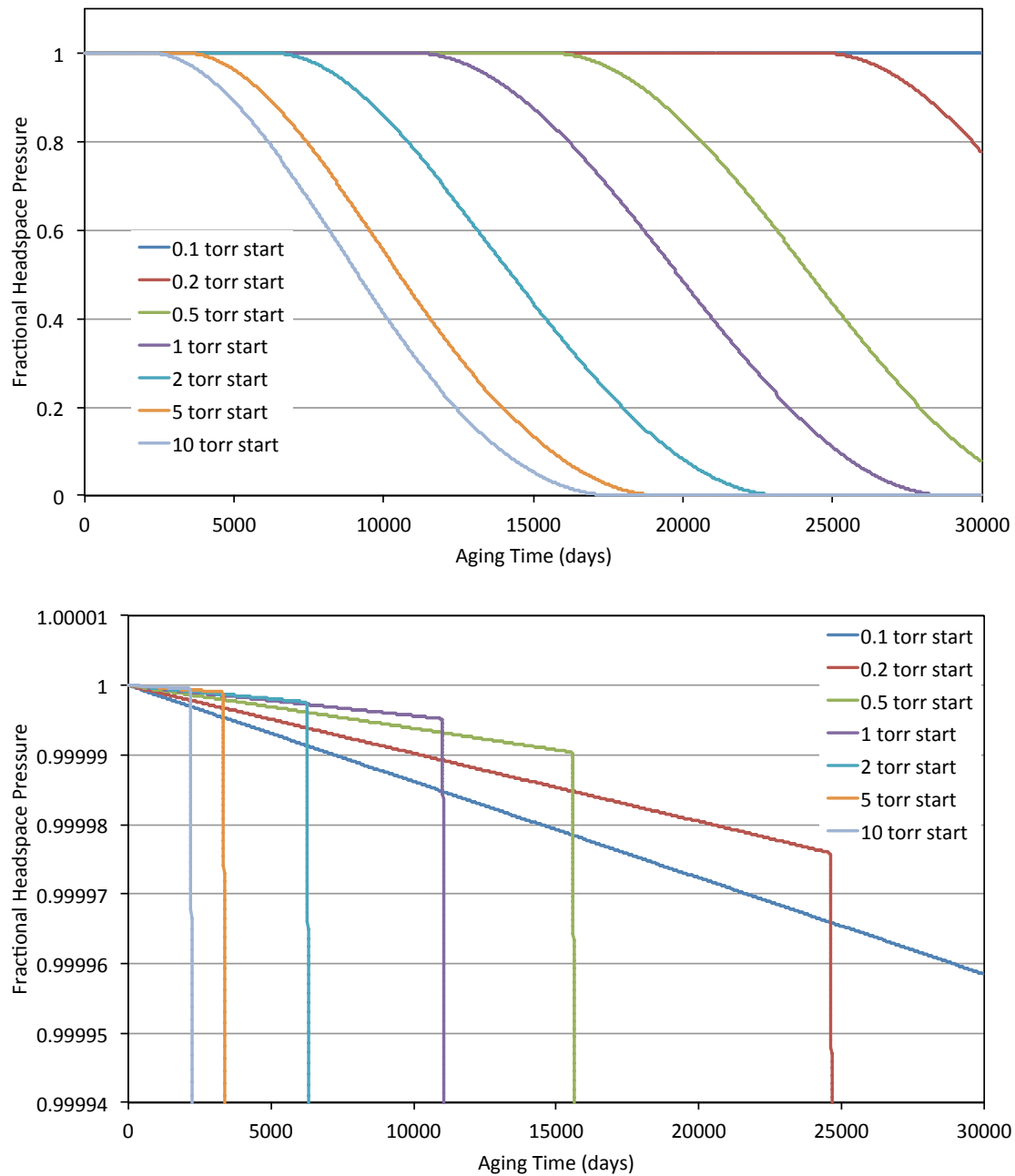


Figure 8. Sensitivity examination for the gas reactor simulation using the model. The analysis shows fractional headspace pressure as a function of aging time. In this case the “standard” parameters are $0.001 \mu\text{m}^2$ defect site area, $30 \mu\text{m}$ nucleation depth, 500 cm^3 reactor volume, 100 nucleation sites, and variable starting hydrogen pressure. The top plot shows complete behavior through the break-through and bulk hydride growth kinetics. The bottom plot shows an expanded region of only the subsurface growth (induction period) phase.

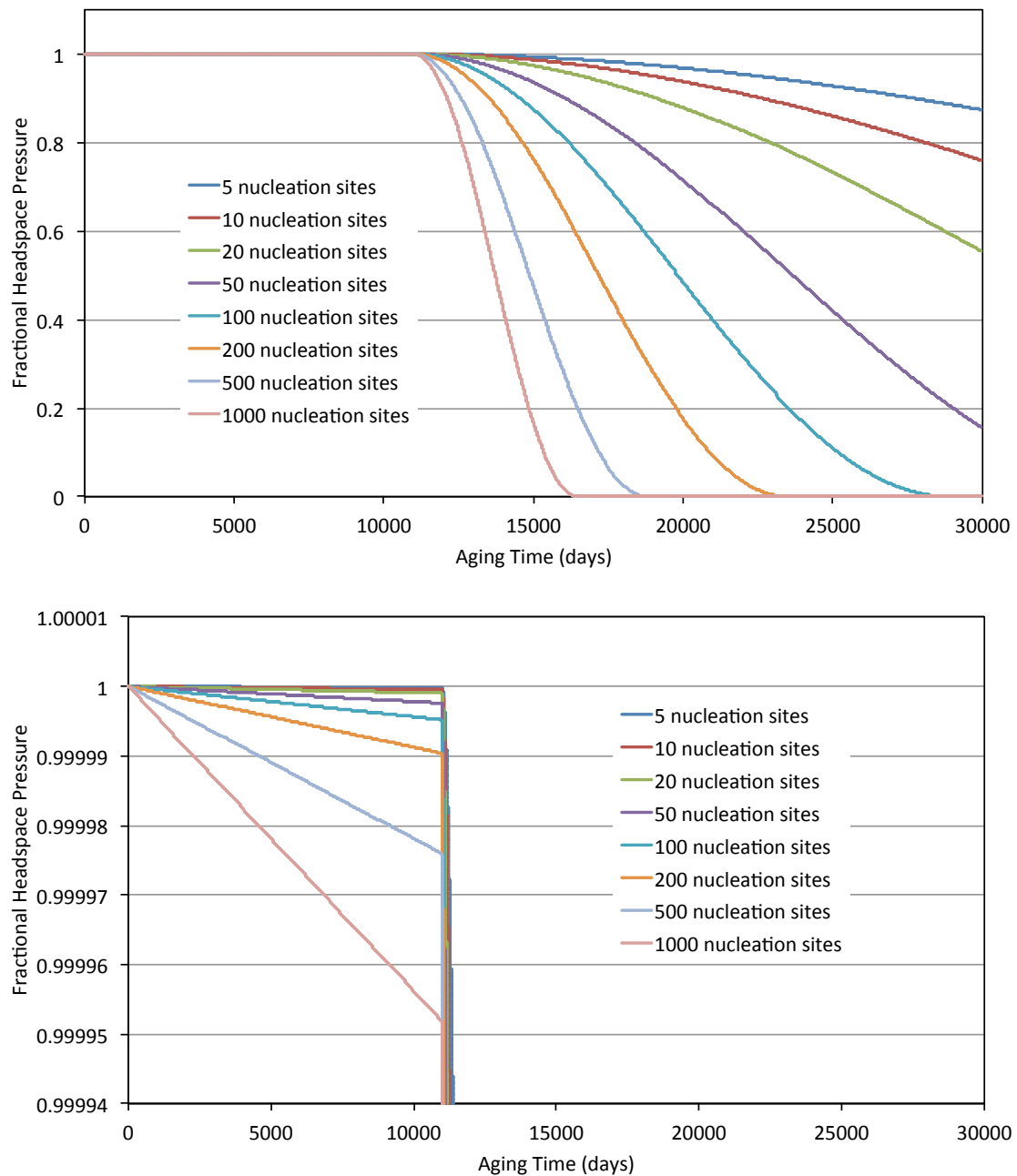


Figure 9. Sensitivity examination for the gas reactor simulation using the model. The analysis shows fractional headspace pressure as a function of aging time. In this case the “standard” parameters are $0.001 \mu\text{m}^2$ defect site area, $30 \mu\text{m}$ nucleation depth, 500 cm^3 reactor volume, 1 torr H_2 start pressure, and variable number of nucleation sites. The top plot shows complete behavior through the break-through and bulk hydride growth kinetics. The bottom plot shows an expanded region of only the subsurface growth (induction period) phase.

There are a limited number of gas reactor experiments to which the model can be compared in order to help calibrate adjustable parameters in the model.

Unfortunately the gas pressure data from the Enhanced Surveillance Parametric Hydriding Study cannot be used for this. There are several problems. The stability and resolution of the gauges used in this study was not great enough to produce high fidelity data. Furthermore, the hydrogen in the reactor cells was a very small fraction ($<2.5\%$) of the total pressure in the cell with the balance being He. There is a chance analysis might be done with the 15 torr and 50 torr special sample cells using time dependent pressure data and time dependent image data to identify break-through times and subsequent further growth of hydride volume. We have a number of other gas reactor hydriding experiments performed at relevant conditions, but with specially prepared uranium surfaces that are unlike engineering surfaces. These are highly polished surfaces of high purity uranium that were carefully cleaned by ion sputtering and annealing, and have a surface oxide grown through pure O_2 exposure at 120 torr (oxygen partial pressure at Los Alamos altitude). Nevertheless, a comparison to the model is in order. This comparison is shown in figure 10.

Figure 10. shows experimental fractional reactor pressure as a function of aging time (exposure time to pure deuterium gas) of the uranium surface for two experiments – one performed at a 1.0 torr starting pressure, and the other at a 2.0 torr starting pressure. The experimental pressure data is shown as broad colored lines. The reactor pressure data is of high fidelity and resolution, however there is no image data to go along with this set of data to identify the break-through time, the number of hydride nuclei, and the further growth of corrosion product. The model provides an excellent fit to the experimental data. The fits are shown as thin solid black lines and lay directly on top of the experimental data. This indicates that the model as formulated has very good physical relevance to the engineering hydriding situation as expressed through the 10-step mechanism. The parameters used to make this fit, however, are physically unrealistic for the engineering case. This is a result of the special surface preparation in these experiments which were designed to foster initiation of a hydriding reaction in a relatively short time. In particular the number of hydride nuclei are very high ($\sim 10^6$) and the starting defect area for ingress is also large ($\sim 500 \mu m^2$). For this experiment, this is understood as the majority of the $\sim 0.5 \text{ cm}^2$ uranium surface being activated for hydriding, with each oxide grain of the thin film acting as an ingress point for hydrogen. Note that the time evolution of the fractional gas pressure for the two experiments (1.0 and 2.0 torr) does not match that expected from the analysis in figure 8. The expectation in this model analysis is that a higher pressure will ultimately lead to earlier break-through time and quicker depletion of the hydrogen available in the reactor. This is

not the case for the experiments, indicating that the two sample surfaces were sufficiently different (numbers of hydride nuclei and area of ingress defect) to reverse the expected result.

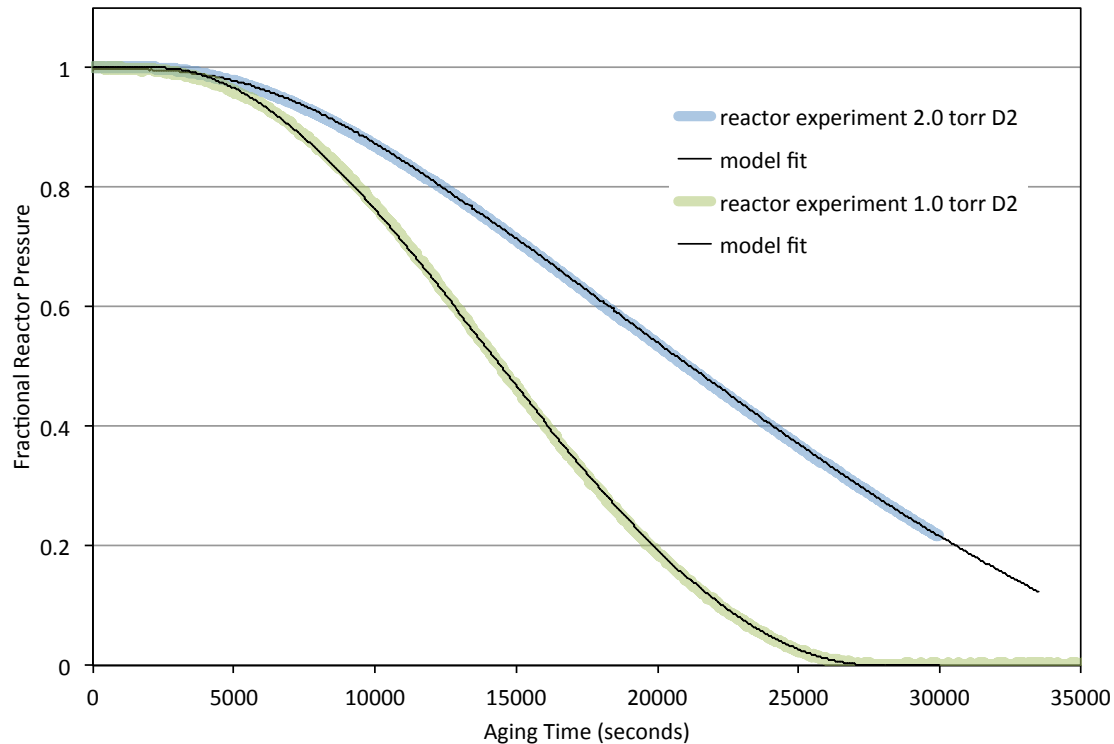


Figure 10. Two sets of experimental gas reactor hydriding data (broad colored lines) with fits from the model developed here (thin black lines). These experiments were performed in a UHV reactor of $\sim 730 \text{ cm}^3$ volume with specially prepared high purity uranium surfaces (not engineering material). Note that the fit of the experimental data by the model is excellent, indicating that for these surfaces and conditions the model provides an accurate description of the hydriding process. See text for discussion.

Experimental Project to Provide Model Calibration

In order to provide proper calibration for this model (or any other hydriding model) there is a set of experimental gas reactor measurements that need to be made. First, it is important to understand what is possible to measure and what is required to calibrate a model. Second, the sample surface needs to be carefully prepared in order to duplicate the engineering case and possibly with additional highly polished surfaces to provide better imaging fidelity. And third, the measurements need to be made under conditions of engineering relevance.

1) Reactor and measurements

- a. Gas reactor cell with high resolution and accuracy pressure measurement (differential capacitance manometer)

- b. Precision measurement of reactor volume
 - c. High-magnification, high resolution imaging of sample surface in order to detect total numbers of nuclei, break-through times, and further growth of hydride volume
 - d. Clean source of hydrogen (hydrogen purifier or metal hydride bed)
- 2) Sample surface
- a. Engineering relevant uranium material
 - b. Surface finish to duplicate relevant conditions or to study specific aspects of factors influencing the mechanism
 - c. Bottom and all sides and edges passivated towards hydriding so that hydriding only takes place on the surface that is imaged
 - d. Possibly some experiments with highly polished surfaces required in order provide better imaging fidelity for break-through time and counting numbers of hydride nuclei
- 3) Measurements of relevance
- a. Hydriding experiments with neat hydrogen and also gas mixtures
 - b. Starting hydrogen pressures in range of 0.01 to 10 torr of hydrogen
 - c. Ambient temperatures or otherwise to understand temperature dependence

For a given experiment, the following data needs to be collected in order to provide proper validation and calibration for a model:

- Reactor pressure as a function of time (yields moles of hydrogen consumed)
- Temperature
- Total numbers of nuclei (and distribution as a function of time)
- Time of nuclei break-through (and the distribution as a function of time)
- Hydride volume growth (rate) as a function of time after break-through
- Hydrogen consumed in reaction if isobaric experiment is performed

The model will have the following variable parameters:

- Starting hydrogen pressure – set as a variable to match experiment
- Defect starting area (will be a distribution) – adjustable parameter to be calibrated
- Depth of nucleation site (will be a distribution) – adjustable parameter to be calibrated
- Reactor volume – set as a variable to match experiment
- Number of nucleation sites (will be a distribution with time) – determined through imaging in the experiment

The model should correctly be able to predict:

- Reactor hydrogen pressure decrease as a function of time
- Time to break-through phase
- Further volume evolution of hydride product after break-through

Summary

We have presented a physically based and geometrically simple model for hydride nucleation and growth at engineering uranium surfaces (oxide thin film covered) based on processes taking place in the 10-step mechanism of hydriding. This model uses two experimentally determined reaction rates – one for hydrogen ingress into the metal surface through a defect location, providing an effective short circuit path for hydrogen past the nominally passivating UO_2 oxide, and the second for hydrogen ingress into the metal through a layer of UH_3 corrosion product, used when the hydrides reach the break-through phase. The output of the model predicts volume growth of the subsurface and later break-through phases of the hydride corrosion product. It also predicts gas consumption as a function of time and pressure as the hydrides grow, as would be measured in a reactor experiment.

In a general sense the predicted behavior fits broad behavior observed experimentally in uranium hydriding with the so called “induction period” exhibiting vanishingly slow growth of hydride product as the subsurface hydride nuclei grow, primarily because the hydrogen ingress rate is very small, and then much faster and accelerating growth of corrosion product at and beyond the surface break-through of the corrosion product as the hydrogen ingress rate becomes substantially larger due to increasing area of exposure. The model fits some available experimental gas reactor data very well, indicating excellent physical relevance of this model as expressed through the 10-step hydriding mechanism. The model uses two adjustable parameters for evolution of a single hydriding location: defect area available for hydrogen ingress in the subsurface growth phase and original depth into the surface of the initial nucleation site. These are both important in the induction period of hydride growth and are required to predict the break-through time and the hydride growth evolution after break-through. A third adjustable parameter of number of (identical) nucleation sites is required to simulate reactor gas consumption data for coupon-type experiments.

There is a very good possibility that this model could be calibrated and validated for engineering uranium surfaces through a couple of avenues. First, a more careful image analysis of data associated with the ESC Parametric Study should yield a measure (distribution) of break-through times, an estimate (distribution) of nucleation depths from the hydride sizes just after break-through, and an estimate

of hydride product volume growth past the break-through phase. Second, a carefully planned gas reactor experimental campaign should be performed that measures identically the output of the model. This should include imaging of the surface as a function of aging time to yield break-through times, nucleation depths, and growth past break-through, in conjunction with measured gas consumption rates. With this comprehensive set of data, the model parameters may be calibrated for engineering uranium surfaces for a variety of pressure conditions.

Additional models of importance and future work

For models employing much more fidelity and mathematical rigor, the reader is directed to several recent manuscripts by J. Glascott (“A model for the initiation of reaction sites during the uranium-hydrogen reaction assuming enhanced hydrogen transport through thin areas of surface oxide”, *Phil. Mag.*, 94, 221-241 (2014), and “A model for the initiation of reaction sites during the uranium-hydrogen reaction assuming enhanced hydrogen transport through linear oxide discontinuities”, *Phil. Mag.*, 94, 1393-1413 (2014)). This work is the culmination of several decades of study of this topic by the author. These models deal with the processes occurring in every step of the 10-step mechanism a detailed physical sense, where the model described here uses overall measured reaction rates and geometric simplicity to capture those fine details. Note that the description of “enhanced hydrogen transport” by Glascott fits identically with the concept of hydrogen ingress into the surface through existing surface defects used in the model developed here. There is increased geometric fidelity employed by Glascott by specifying the nature and spatial definition of those transport locations.

More recently Phil Monks, et al. of AWE have developed a stochastic model based on the formalism described here. This model successfully describes the large data set of uranium hydriding coupon experiments generated by AWE over the past 10 years. The model uses a limited set of adjustable parameters and finds a best fit for these through linear least squares fitting. Some differences include a $P^{2/3}$ dependence of the reaction rate on pressure rather than a $P^{1/2}$ dependence as the model here suggests. More details will be forthcoming on this model in the near future.

Future work on refining this mechanistic model will incorporate information from several sources. As additional work is performed here at Los Alamos and elsewhere, there is additional fidelity in understanding the fine details of the hydriding mechanism. In particular, the Uranium Corrosion LDRD ER currently ongoing is examining the very early stage (mechanism steps 3-7) nucleation and growth of the hydride product. In this early stage of nucleation and growth the hydride product is clearly not spherical, but rather finds lines of weakness (grain boundaries, twin-

boundaries, inclusion-metal interfaces) along which to grow. This will ultimately need to be a refinement in the improved mechanistic model. Additionally, the High Sensitivity Reactor (HSR) capability developed by the author under the Aging and Lifetimes program at LANL is being used for high fidelity coupon experiments for model comparison and validation.

Key questions that need to be addressed in future work to refine our understanding of the hydriding mechanism have been listed above and are reiterated here:

- 1) Specific chemical or structural nature of the preferred subsurface nucleation site(s)
- 2) Role of the specific nature of the surface of the U metal (e.g. presence and thickness of a work hardened metal layer, nature of surface oxide) and how this affects the specific mechanism
- 3) Nature of the surface defect site(s) allowing hydrogen ingress
- 4) Effective area (kinetic effect during incubation period) of the defect site at the surface available for hydrogen ingress
- 5) Original depth of the subsurface nucleation site (or distribution), and the critical depth required for arrested growth of the hydride nucleus

Acknowledgements

This work was made possible primarily through the support of the LANL Enhanced Surveillance program (now known as the Aging and Lifetimes program). The experimental efforts that helped inform this work took place over a period of approximately 10 years, primarily in the Surface Science Laboratory capability which was set up by the author in the Materials Science Laboratory building in MST Division. The author would like to acknowledge contributions and valuable discussion from Robert Hanrahan, Louis Powell, Wigbert Siekhaus, Robert Harker, James Petherbridge, Phil Monks, Joe Glascott, Thomas Taylor, Debra Johnson, Cyril Opeil, John Tanski, Mark Paffett, Edward Holby, Andrew Richards, and others.